

Analyses of Type Ia Supernova Data in Cosmological Models with a Local Void

Kenji TOMITA^{*)}

Yukawa Institute for Theoretical Physics, Kyoto University, Kyoto 606-8502

(Received)

The data of type Ia supernovae observed by the High- z SN Search Team and Supernova Cosmology Project are analyzed in inhomogeneous cosmological models with a local void on scales of about 200 Mpc, to derive the best-fit values of model parameters and the confidence contours. The χ^2 fitting is found to be slightly better than that in homogeneous models. It is shown that (1) the best-fit values are most sensitive to the ratio R of the outer Hubble constant (H_0^{II}) to the inner Hubble constant (H_0^{I}), (2) the best-fit outer density parameter (Ω_0^{II}) (and cosmological constant parameter (λ_0^{II})) increases (and decreases) with the increase of R , respectively, and (3) ($\Omega_0^{\text{II}}, \lambda_0^{\text{II}}$) can be (1, 0) for $R \approx 0.8$. Moreover it is shown that these models may be naturally consistent with the new supernova data (SN1997ff) for $z = 1.7$.

§1. Introduction

Nowadays the most important cosmological observations are the [magnitude m - redshift z] relation of type Ia supernovae (SNIa) and the CMB anisotropy. In the former observations, SNIa play a role of best standard candles and two groups, the High- z SN Search Team^{1), 2), 3)} and the Supernova Cosmology Project⁴⁾ have so far observed 50 and 60 SNIa, respectively. From their results it was suggested that a significant dark energy content fills our universe under the assumption of its homogeneity and isotropy.

On the other hand, inhomogeneous models with a local void on scales of about 200 Mpc were studied by the present author⁵⁾ in connection with the puzzling behavior of cosmic bulk flows^{6), 7)}, and the possibility that the accelerating behavior of high- z SNIa in $[m, z]$ relation may be explained without cosmological constant was shown subsequently⁸⁾. A historical survey of works concerned with local voids can be seen in one of previous papers⁹⁾. Since these inhomogeneous models include many parameters (such as the inner and outer values of the Hubble constant and density parameter, cosmological constant and the boundary radius), we have recently examined the dependence of the above relation on these parameters, in comparison with the relations in homogeneous models with $(\Omega_0, \lambda_0) = (0.3, 0.7)$ and $(0.3, 0.0)$ ¹⁰⁾.

From the observational viewpoint, recent galactic redshift surveys^{11), 12), 13), 14)} show that in the region around $200 - 300h^{-1}$ Mpc from us the distribution of galaxies may be inhomogeneous. Moreover, a large-scale inhomogeneity suggesting a wall around the void on scales of $\sim 250h^{-1}$ Mpc has recently been found by Blanton et al.¹⁵⁾ in the SDSS commissioning data. Similar walls on scales of $\sim 250h^{-1}$ Mpc have already been found in the Las Campanas and 2dF redshift surveys near the

^{*)} E-mail address: tomita@yukawa.kyoto-u.ac.jp

Northern and Southern Galactic Caps^{16), 13), 17)}. These results may mean that there is a local void with the radius of $200 - 300h^{-1}$ Mpc and we live in it.

In this paper we analyze directly the SNIa data of the above two groups in our inhomogeneous models with a local void on scales of about 200 Mpc, and show the confidence contours as well as the best-fit values of the model parameters. In §2 we give the basic formulation of distance modulus and the χ square for statistical fitting. In §3 show the best-fit values of model parameters and confidence contours. Moreover we compare the behavior of our models with the new data for $z = 1.7$,¹⁸⁾ and find that they may be naturally consistent with it. In §4 discussions and concluding remarks are described.

§2. Distance modulus and the χ square

The theoretical distance modulus is defined by

$$\mu_0^p = 5 \log \left(d_L / \text{Mpc} \right) + 25, \quad (2 \cdot 1)$$

where d_L is the luminosity distance related to the angular-diameter distance d_A by

$$d_L = (1 + z)^2 d_A \quad (2 \cdot 2)$$

along the light ray to a source S with the redshift z . This distance modulus is compared with the observed one given by

$$\mu_0 = m_B - M_B, \quad (2 \cdot 3)$$

where M_B and m_B are the peak absolute magnitude and the corresponding apparent magnitude of a standard SNIa in the B band, respectively.

In this paper we consider spherical inhomogeneous cosmological models which consist of the inner homogeneous region (V^I) and the outer homogeneous region (V^{II}) with the boundary of radius ~ 200 Mpc. The observer's position O deviates generally from the center C, but is assumed to be comparatively close to C. For the off-center observer, the angular-diameter distance d_A depends not only on z , but also the angle between the vectors \overline{CO} and \overline{CS} , where S is the source. In our previous papers^{5), 8)} the behavior of distances for off-center observers was studied. Since the angular dependence is small for remote sources, however, we can neglect it for simplicity, assuming that we are approximately at the center. Then d_A depends on the source redshift z , the inner and outer Hubble constants H_0^I and H_0^{II} , the inner and outer density parameters Ω_0^I and Ω_0^{II} , the outer Λ parameter λ_0^{II} , and the boundary redshift z_1 . The inner Λ parameter λ_0^I is related to λ_0^{II} by $\lambda_0^I = \lambda_0^{II} (H_0^{II}/H_0^I)^2$. The equation to be solved for deriving d_A and the junction conditions were shown in Eqs. (5) - (11) in a previous paper¹⁰⁾.

The best-fit values of the cosmological parameters are determined using the χ square :

$$\chi^2 = \sum_i \left[\mu_{0,i}^p (z_i | H_0^I, H_0^{II}, \Omega_0^I, \Omega_0^{II}, \lambda_0^{II}, z_1) - \mu_{0,i} \right]^2$$

$$/(\sigma_{\mu 0,i}^2 + \sigma_{mz,i}^2), \quad (2.4)$$

where $\sigma_{\mu 0}$ is the measurement error of the distance modulus and σ_{mz} is the dispersion in the distance modulus corresponding to the dispersion of galaxy redshift σ_z (coming from peculiar velocity and uncertainty). σ_{mz} is related to σ_z as

$$\sigma_{mz} = \frac{5}{\ln 10} \left(\frac{1}{d_L} \frac{\partial d_L}{\partial z} \right). \quad (2.5)$$

Next the probability distribution function (PDF) is necessary to derive the confidential contours as well as the most likely values of model parameters. It is expressed as

$$p(H_0^I, H_0^{II}, \Omega_0^I, \Omega_0^{II}, \lambda_0^{II}, z_1 | \mu_0) \propto \exp(-\frac{1}{2} \chi^2), \quad (2.6)$$

which is consistent with Eq.(9) in Riess et al.²⁾.

In the present inhomogeneous models there are six parameters and it is too complicated to consider all of them at the same time. So we treat here several cases with specific values of $z_1, H_0^{II}/H_0^I$, and Ω_0^I . Then the corresponding normalized PDF is expressed as

$$p(H_0^I, \Omega_0^{II}, \lambda_0^{II} | \mu_0) = \frac{\exp(-\frac{1}{2} \chi^2)}{\int_{-\infty}^{\infty} dH_0^I \int_{-\infty}^{\infty} d\lambda_0^{II} \int_{\Omega_{0l}}^{\infty} \exp(-\frac{1}{2} \chi^2) d\Omega_0^{II}} \quad (2.7)$$

for given $z_1, H_0^{II}/H_0^I$, and Ω_0^I , where μ_0 is the used set of distance moduli and Ω_{0l} is the assumed lower limit of Ω_0^{II} , being 0 or $-\infty$. Physically the region of $\Omega_0^{II} < 0$ is meaningless, while it is significant statistically. To see the probability distribution independent of H_0^I , we can consider the following quantity:

$$p(\Omega_0^{II}, \lambda_0^{II} | \mu_0) = \int_{-\infty}^{\infty} p(H_0^I, \Omega_0^{II}, \lambda_0^{II} | \mu_0) dH_0^I. \quad (2.8)$$

The contours are drawn due to $p(\Omega_0^{II}, \lambda_0^{II} | \mu_0)$.

§3. Supernova data and the fitting

At present we have two SNIa data to be used for determining cosmological parameters: data of HSST (Schmidt et al.¹⁾; Riess et al.²⁾) with 50 SNIa, and the data of SCP (Perlmutter et al.⁴⁾) with 60 SNIa. 18 SNIa are common to both data.

In the former, there are two types of μ_0 data : data due to the Multicolor Light Curve Shape method (MLCS) and the template-fitting method. In each method we can use the data of $z_i, \mu_{0,i}$ and $\sigma_{\mu 0,i}$ (for $i = 1 - 50$) given in their Tables. Following Riess et al.²⁾ for σ_z , we adopt $\sigma_z = 200 \text{ km s}^{-1}$ and add 2500 km s^{-1} in quadrature to σ_z for SNIa whose redshifts were determined from broad features in the SN spectrum.

In Perlmutter et al.'s paper, the data of $m_{B,i}^{\text{eff}}, z_i, \sigma_{mz,i}$ and $\sigma_{z,i}$ ($i = 1 - 60$) were shown, but the direct values of $\mu_{0,i}$ were not published and cannot be used. As was shown by Wang¹⁹⁾, however, we have for 18 SNIa common to two teams

$$M_B^{\text{MLCS}} \equiv m_B^{\text{eff}} - \mu_0^{\text{MLCS}} = -19.33 \pm 0.25, \quad (3.1)$$

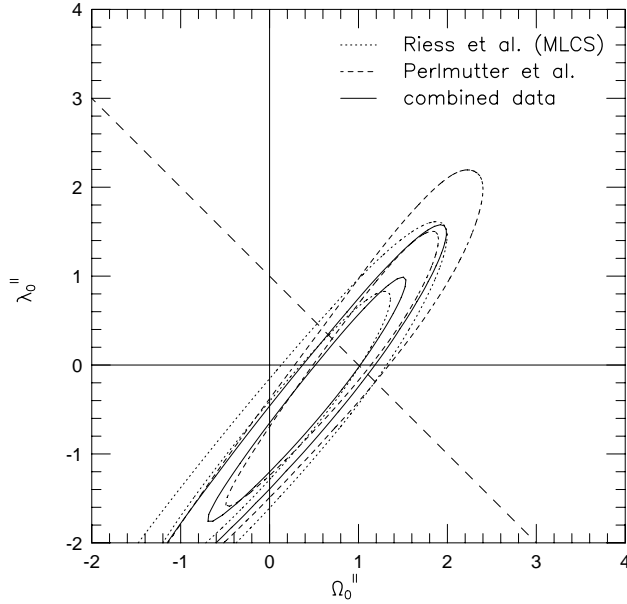


Fig. 1. 68.3 % and 95.4 % confidence contours in the $\Omega_0^{\text{II}} - \lambda_0^{\text{II}}$ plane in the case of $(z_1, H_0^{\text{II}}/H_0^{\text{I}}, \Omega_0^{\text{I}}) = (0.080, 0.82, \text{A})$. The dotted lines represent the Riess et al. (1998) data, the dashed lines represent the Perlmutter et al (1999) data, and the solid lines represent the combined data.

where m_B^{eff} is the effective B-band magnitude of SNIa given by Perlmutter et al., and μ_0^{MLCS} is the corresponding data of μ_0 due to MLCS method in Riess et al.²⁾.

For the corrected B-band peak absolute magnitude given by Hamuy et al.²⁰⁾, on the other hand, we have

$$M_B^{\text{MLCS}} - M_B^{\text{H96}} = -0.047 \pm 0.270 \quad (3.2)$$

which is small enough, compared with the counterpart due to the template-fitting method. Accordingly we adopt the MLCS data among Riess et al. two data, and derive the values of μ_0 in Perlmutter et al.'s data using the relation

$$\mu_0 = m_B^{\text{eff}} - \bar{M}_B \text{ with } \bar{M}_B = -19.33 \quad (3.3)$$

following Wang¹⁹⁾.

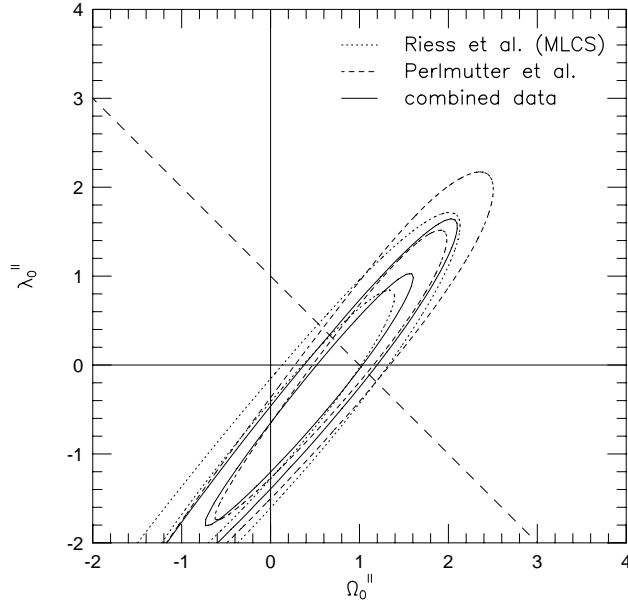


Fig. 2. 68.3 % and 95.4 % confidence contours in the $\Omega_0^{\text{II}} - \lambda_0^{\text{II}}$ plane in the case of $(z_1, H_0^{\text{II}}/H_0^{\text{I}}, \Omega_0^{\text{I}}) = (0.080, 0.82, \text{B})$.

From the two data sets we can make a combined data consisting of 50 SNIa (from Riess et al.) and 42 SNIa (from Perlmutter et al.), where Riess et al. data are used for 18 common data (due to Wang's procedure¹⁹⁾).

The above three kinds of data are compared with the theoretical models with the following conditions about z_1 , $H_0^{\text{II}}/H_0^{\text{I}}$, and Ω_0^{I} . For z_1 , we adopt mainly $z_1 = 0.080$ corresponding to the radius $240/h^{\text{I}}$ Mpc, where $H_0^{\text{I}} = 100h^{\text{I}}$ km s⁻¹ Mpc⁻¹, and compare PDF in this case later with PDF in cases with $z_1 = 0.067$ ($cz_1/H_0^{\text{I}} = 200/h^{\text{I}}$ Mpc) and $0.100(300/h^{\text{I}}$ Mpc). For $H_0^{\text{II}}/H_0^{\text{I}}$, we consider three cases with $H_0^{\text{II}}/H_0^{\text{I}} = 0.80, 0.82$ and 0.87 or $H_0^{\text{I}}/H_0^{\text{II}} = 0.25, 1.20$ and 1.15 , respectively.

For Ω_0^{I} , we adopt firstly the inner low-density case (A) in which

$$\Omega_0^{\text{I}} = 0.3 \quad \text{for } \Omega_0^{\text{II}} > 0.6 \quad (3.4)$$

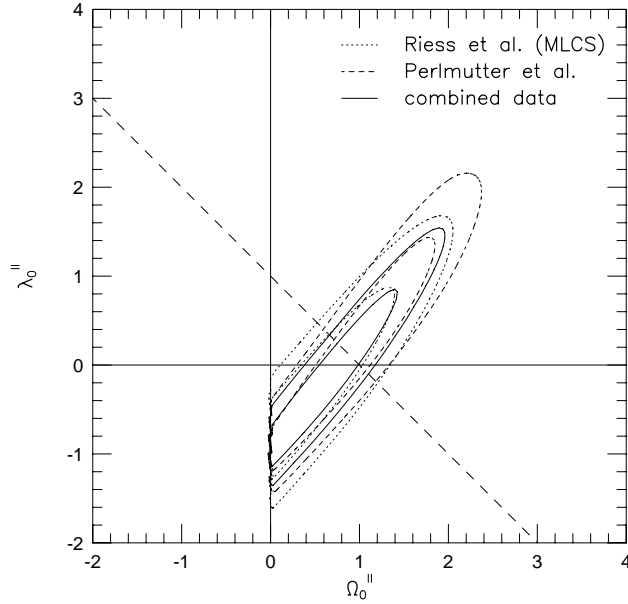


Fig. 3. 68.3 % and 95.4 % confidence contours in the $\Omega_0^{\text{II}} - \lambda_0^{\text{II}}$ plane in the case of $(z_1, H_0^{\text{II}}/H_0^{\text{I}}, \Omega_0^{\text{I}}) = (0.080, 0.82, \text{A})$ with $\Omega_{0l} = 0$.

and

$$\Omega_0^{\text{I}} = \Omega_0^{\text{II}}/2 \quad \text{for } \Omega_0^{\text{II}} < 0.6. \quad (3.5)$$

For a comparison we consider the equi-density case (B) with

$$\Omega_0^{\text{I}} = \Omega_0^{\text{II}} \left(H_0^{\text{II}}/H_0^{\text{I}} \right)^2. \quad (3.6)$$

Since $\rho_0^j \propto (H_0^j)^2 \Omega_0^j$ ($j = \text{I}, \text{II}$), we have $\rho_0^{\text{I}} = \rho_0^{\text{II}}$ in this case.

In Figures 1, 2, 3, 4 and 5, we show the 68.3 % and 95.4 % confidence contours in the $\Omega_0^{\text{II}} - \lambda_0^{\text{II}}$ plane. In Figures 1, 2 and 3, we use three kinds of data and treat the three cases in which $(z_1, H_0^{\text{II}}/H_0^{\text{I}}, \Omega_0^{\text{I}}) = (0.080, 0.82, \text{A})$, $(0.080, 0.82, \text{B})$, and $(0.080, 0.82, \text{A})$ with $\Omega_{0l} = 0$, respectively. Only in the case with $\Omega_{0l} = 0$, the region of $\Omega_0^{\text{II}} < 0$ is excluded. It is found comparing these figures that the difference

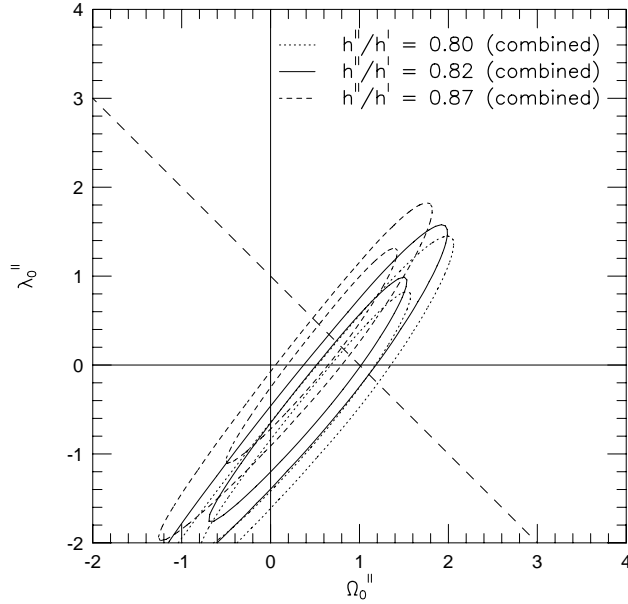


Fig. 4. 68.3 % and 95.4 % confidence contours in the $\Omega_0^{\text{II}} - \lambda_0^{\text{II}}$ plane for the combined data. The dotted lines, solid lines and dashed lines represent the cases of $H_0^{\text{II}}/H_0^{\text{I}} = 0.80, 0.82$, and 0.87 , respectively.

between two cases A and B is small, and similarly the difference between two cases with $\Omega_{0l} = -\infty$ and 0 is also small.

In Figs. 4 and 5, we show the difference in the contours in the cases with $R \equiv H_0^{\text{II}}/H_0^{\text{I}} = 0.80, 0.82$ and 0.87 and $z_1 = 0.067, 0.080$ and 0.100 , respectively, using the combined data. It is interesting that, as R decreases, the contours move to the direction of larger Ω_0^{II} and smaller λ_0^{II} , and for $R = 0.80$ the flat case with vanishing cosmological constant (the Einstein-de Sitter model) can be at the center of the contours.

In Table I the best-fit values of cosmological parameters in homogeneous models are listed for a later comparison. In Table II, III and IV, we show the best-fit values of h^{I} , Ω_0^{II} and λ_0^{II} with 1σ error bars, and the corresponding χ^2_{ν} in cases of $H_0^{\text{II}}/H_0^{\text{I}} = 0.82, 0.87$ and 0.80 , respectively, assuming $z_1 = 0.080$ and Ω_0^{I} (A). The

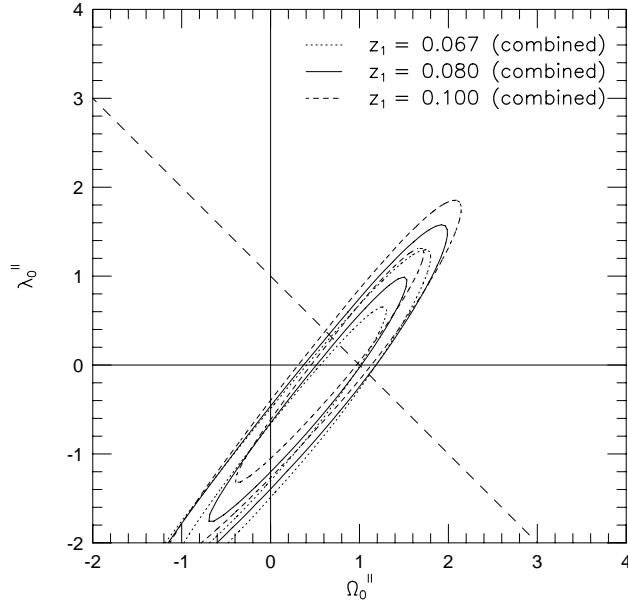


Fig. 5. 68.3 % and 95.4 % confidence contours in the $\Omega_0^{\text{II}} - \lambda_0^{\text{II}}$ plane for the combined data. The dotted lines, solid lines and dashed lines represent the cases of $z_1 = 0.067, 0.080$, and 0.100 , respectively.

Table I. Determined model parameters in homogeneous models. χ_{ν}^2 is χ^2 per degree of freedom. $H_0 = 100h \text{ km s}^{-1} \text{ Mpc}^{-1}$. The errors of h represent only statistical ones.

data	Riess et al.	Perlmutter et al.	combined
h	0.65 ± 0.01	0.666 ± 0.02	0.65 ± 0.01
Ω_0	0.2 ± 0.6	1.0 ± 0.4	0.7 ± 0.4
λ_0	0.7 ± 0.8	1.7 ± 0.6	1.2 ± 0.5
χ_{ν}^2	1.11	1.57	1.45

error bars of h^{I} include only statistical errors, but not the contribution from the errors of absolute magnitudes. χ_{ν}^2 in Perlmutter et al. data is found to be much larger than that in Riess et al. data. This comes from the situation that we made artificially their data of μ_0 assuming the average absolute magnitude. In Riess et al. data, χ_{ν}^2 in our inhomogeneous models is smaller than that in homogeneous

Table II. Determined model parameters in the case of $(z_1, H_0^{\text{II}}/H_0^{\text{I}}, \Omega_0^{\text{I}}) = (0.080, 0.80, \text{A})$. χ_{ν}^2 is χ^2 per degree of freedom. $H_0^{\text{I}} = 100h^{\text{I}} \text{ km s}^{-1} \text{ Mpc}^{-1}$. The errors of h^{I} represent only statistical ones.

data	Riess et al.	Perlmutter et al.	combined
h^{I}	0.64 ± 0.01	0.64 ± 0.02	0.64 ± 0.01
Ω_0^{II}	0.1 ± 0.7	0.9 ± 0.6	0.5 ± 0.5
λ_0^{II}	-0.9 ± 1.0	-0.1 ± 0.8	-0.5 ± 0.7
χ_{ν}^2	1.05	1.62	1.42
$(\Omega_0^{\text{II}})_{\text{flat}}$	1.0 ± 0.2	1.0 ± 0.2	1.0 ± 0.1

Table III. Determined model parameters in the case of $(z_1, H_0^{\text{II}}/H_0^{\text{I}}, \Omega_0^{\text{I}}) = (0.080, 0.82, \text{A})$. χ_{ν}^2 is χ^2 per degree of freedom. $H_0^{\text{I}} = 100h^{\text{I}} \text{ km s}^{-1} \text{ Mpc}^{-1}$. The errors of h^{I} represent only statistical ones.

data	Riess et al.	Perlmutter et al.	combined
h^{I}	0.64 ± 0.01	0.64 ± 0.02	0.64 ± 0.01
Ω_0^{II}	0.1 ± 0.7	0.9 ± 0.7	0.6 ± 0.5
λ_0^{II}	-0.7 ± 1.1	0.1 ± 1.0	-0.2 ± 0.7
χ_{ν}^2	1.05	1.61	1.42
$(\Omega_0^{\text{II}})_{\text{flat}}$	0.9 ± 0.2	0.9 ± 0.2	0.9 ± 0.1

models (Table 1) and so this data are more fitted to our inhomogeneous models or the inhomogeneity of Hubble constant, though many parameters are included in our case. To the bottom of Tables II - V, we add $(\Omega_0^{\text{II}})_{\text{flat}}$, the density parameter in the case when the outer region is spatially flat.

In Table V we show the best-fit values in the case of Ω_0^{I} (B), assuming $H_0^{\text{II}}/H_0^{\text{I}} = 0.82$, $z_1 = 0.080$. From comparison between Table II and Table V, the best-fit values are not sensitive to Ω_0^{I} . In Table VI, moreover, we show the cases with $z_1 = 0.067$ and 0.100 assuming $H_0^{\text{II}}/H_0^{\text{I}} = 0.82$ and Ω_0^{I} (A). It is found from this Table that, because of the smallest χ_{ν}^2 , the fitting for $z_1 = 0.080$ is best, compared with the cases with $z_1 = 0.067$ and 0.100. This result may be connected with the situation that the boundary radius of the observed local void is likely to be between $200/h^{\text{I}}$ Mpc and $300/h^{\text{I}}$ Mpc.

Finally we compare the behavior of our models with the new supernova data for $z = 1.7$.¹⁸⁾ In Fig. 6 we show the $\Delta(m - M) - \log z$ diagram, where $\Delta(m - M)$ is the difference of $m - M$ in each model from that in the empty homogeneous model ($\Omega_0 = \lambda_0 = 0$). Here we adopted two models with a local void : $(\Omega_0^{\text{II}}, \lambda_0^{\text{II}}) = (1.0, 0.0)$ and $(0.6, 0.0)$. In both models we use $\Omega_0^{\text{I}} = 0.3$, $\lambda_0^{\text{I}} = 0$ and $z_1 = 0.067$ as the other parameters, to which the behavior of the models is not sensitive. The upper, middle and lower curves in each model are for R ($\equiv H_0^{\text{II}}/H_0^{\text{I}}$) = 0.80, 0.82 and 0.87, respectively. For comparison we show the behavior of three homogeneous models : $(\Omega_0, \lambda_0) = (0.35, 0.65)$, $(0.35, 0.0)$ and $(1.0, 0.0)$, and depict in the diagram the binned data ($z < 1$) and the new data (SN 1997ff) for $z = 1.7$, which were given in Fig. 11 of Riess et al.¹⁸⁾ It is found from Fig. 6 that our models may be consistent with the new data in contrast to the flat homogeneous model with $(\Omega_0, \lambda_0) = (0.35, 0.65)$. Especially the model with $(\Omega_0^{\text{II}}, \lambda_0^{\text{II}}) = (1.0, 0.0)$, which is the Einstein-de Sitter model in the external region, seems to naturally accord with all data for $R = 0.80$

and 0.82. In the model with $(\Omega_0^{\text{II}}, \lambda_0^{\text{II}}) = (0.6, 0.0)$, the case $R = 0.87$ is best among three cases. If many data for $z > 1$ are provided, we shall be able to distinguish more clearly the behaviors of the models with a local model and the homogeneous models with dominant cosmological constant or dark energy.

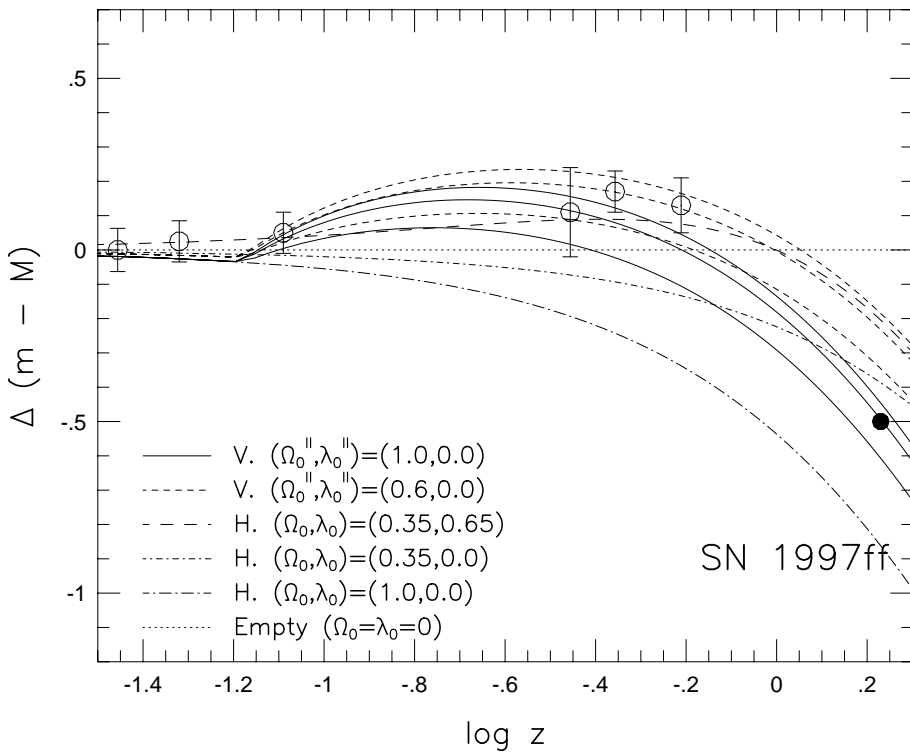


Fig. 6. The $\Delta(m-M)$ – $\log z$ diagram in models with a local void (V) and homogeneous models (H). Here $\Delta(m-M) \equiv (m-M) - (m-M)$ in each model – $(m-M)$ in the empty model ($\Omega_0 = \lambda_0 = 0$). In two (V) models, we have upper, middle and lower curves corresponding to R ($\equiv H_0^{\text{II}}/H_0^{\text{I}}$) = 0.80, 0.82 and 0.87, respectively. For comparison the SNIa binned data ($z < 1$) and the new data of SN 1997ff ($z = 1.7$) are depicted in the diagram.

§4. Concluding remarks

In this paper we derived confidence contours and best-fit parameters in the inhomogeneous models with a local void using the two SNIa data and the combined data, and found that (1) they are very sensitive to the ratio R of the outer Hubble constant (H_0^{II}) to the inner Hubble constant (H_0^{I}), (2) the best-fit outer density parameter (Ω_0^{II}) (and cosmological constant parameter (λ_0^{II})) increases (and decreases) with the increase of R , respectively, and (3) $(\Omega_0^{\text{II}}, \lambda_0^{\text{II}})$ can be $(1, 0)$ for $R \approx 0.8$. Accordingly the existence of our local void may solve the puzzling *cosmological-constant* problem.

However we neglected the directional dependence of $[m, z]$ relation which may be an important factor, especially for nearby SNIa, since magnitudes of SNIa are measured by off-center observers. If the data of angular positions of observed SNIa will be published, the directional dependence can be taken into account and the fitting may be promoted.

The flux averaging proposed by Wang¹⁹⁾ has not been executed here, but it may be important when many high- z data of $z > 1.0$ appear, because they would be much affected by lensing effect.

From a comparison with the new data for $z = 1.7$, we found that our models may be naturally consistent with it, in contrast to the homogeneous models with acceleration due to cosmological constant or dark energy. For $z > 1$ the behavior of curves represents the deceleration of the universe, which depends highly on the equation of state of constituent matter. In our models with a local void it is mainly pressureless matter, while the homogeneous models with dominant cosmological constant and hypothetical dark energy have negative pressure comparable with the mass energy. It is desirous that more data for $z > 1.5$ will be provided in order to distinguish these two types of models more clearly and exclude the fluctuation due to the lensing effect.

Table IV. Determined model parameters in the case of $(z_1, H_0^{\text{II}}/H_0^{\text{I}}, \Omega_0^{\text{I}}) = (0.080, 0.87, \text{A})$. χ_{ν}^2 is χ^2 per degree of freedom. $H_0^{\text{I}} = 100h^{\text{I}} \text{ km s}^{-1} \text{ Mpc}^{-1}$. The errors of h^{I} represent only statistical ones.

data	Riess et al.	Perlmutter et al.	combined
h^{I}	0.64 ± 0.01	0.65 ± 0.02	0.64 ± 0.01
Ω_0^{II}	0.2 ± 1.0	0.7 ± 0.7	0.6 ± 0.6
λ_0^{II}	-0.2 ± 1.1	0.7 ± 1.1	0.3 ± 0.8
χ_{ν}^2	1.05	1.61	1.42
$(\Omega_0^{\text{II}})_{\text{flat}}$	0.7 ± 0.2	0.7 ± 0.2	0.7 ± 0.1

Acknowledgements

The author is grateful to referees for helpful comments. This work was supported by Grant-in Aid for Scientific Research (No. 12440063) from the Ministry of Education, Science, Sports and Culture, Japan.

References

Table V. Determined model parameters in the case of $(z_1, H_0^{\text{II}}/H_0^{\text{I}}, \Omega_0^{\text{I}}) = (0.080, 0.82, \text{B})$. χ_{ν}^2 is χ^2 per degree of freedom. $H_0^{\text{I}} = 100h^{\text{I}} \text{ km s}^{-1} \text{ Mpc}^{-1}$. The errors of h^{I} represent only statistical ones.

data	Riess et al.	Perlmutter et al.	combined
h^{I}	0.64 ± 0.01	0.64 ± 0.02	0.64 ± 0.01
Ω_0^{II}	0.0 ± 0.7	0.8 ± 0.7	0.5 ± 0.5
λ_0^{II}	-0.8 ± 1.1	0.0 ± 1.0	-0.3 ± 0.8
χ_{ν}^2	1.05	1.62	1.42
$(\Omega_0^{\text{II}})_{\text{flat}}$	0.9 ± 0.2	0.9 ± 0.2	0.9 ± 0.1

Table VI. Determined model parameters in the case of $(z_1, H_0^{\text{II}}/H_0^{\text{I}}, \Omega_0^{\text{I}}) = (0.080, 0.82, \text{A})$. χ_{ν}^2 is χ^2 per degree of freedom. $H_0^{\text{I}} = 100h^{\text{I}} \text{ km s}^{-1} \text{ Mpc}^{-1}$. The errors of h^{I} represent only statistical ones.

data	Riess et al.	Riess et al.	combined	combined
z_1	0.067	0.100	0.067	0.100
h^{I}	0.64 ± 0.01	0.64 ± 0.01	0.64 ± 0.01	0.64 ± 0.01
Ω_0^{II}	-0.3 ± 0.7	0.4 ± 0.7	0.2 ± 0.5	0.9 ± 0.5
λ_0^{II}	-1.3 ± 1.1	-0.3 ± 1.1	-0.7 ± 0.8	0.2 ± 0.8
χ_{ν}^2	1.10	1.13	1.45	1.46

- [1] B. P. Schmidt, N. B. Suntzeff, M. M. Phillips, R. A. Schommer, A. Clocchiatti, R. P. Kirshner, P. Garnavich, P. Challis, et al., *Astrophys. J.* **507** (1998), 46.
- [2] A. G. Riess, A. V. Filippenko, P. Challis, A. Clocchiatti, A. Diercks, P. M. Garnavich, R. L. Gilliland, et al., *Astron. J.* **116** (1998), 1009.
- [3] A. G. Riess, A. V. Filippenko, W. Li, B. Schmidt, *Astron. J.* **118** (2000), 2668.
- [4] S. Perlmutter, G. Aldering, G. Goldhaber, R. A. Knop, P. Nugent, D. E. Groom, P. G. Castro, S. Deustua, et al., *Astrophys. J.* **517** (1999), 565.
- [5] K. Tomita, *Astrophys. J.* **529** (2000), 26
- [6] M. J. Hudson, R. J. Smith, J. R. Lucey, D. J. Schlegel, R. L. Davies, *Astrophys. J.* **512** (1999), L79.
- [7] J. A. Willick, *Astrophys. J.* **522** (1999), 647.
- [8] K. Tomita, *Astrophys. J.* **529** (2000), 38.
- [9] K. Tomita, *Prog. Theor. Phys.* **105** (2001), 419.
- [10] K. Tomita, *Mon. Not. R. Astron. Soc.* **326** (2001), 287.
- [11] C. Marinoni, P. Monaco, G. Giuricin, B. Costantini, *Astrophys. J.* **521** (1999), 50.
- [12] R. O. Marzke, L. N. da Costa, P. S. Pellegrini, C. N. A. Willmer, M. J. Geller, *Astrophys. J.* **503** (1998), 617.
- [13] S. Folkes, S. Ronen, I. Price, O. Lahav, M. Colless, S. Maddox, K. Deeley, K. Glazebrook, et al., *Mon. Not. R. Astron. Soc.* **308** (1999), 459.
- [14] E. Zucca, G. Zamorani, G. Vettolani, A. Cappi, R. Merighi, M. Mignoli, H. MacGillivray, C. Collins, C. et al., *Astron. Astrophys.* **326** (1997), 477.
- [15] M. R. Blanton, J. Dalcanton, J. Eisenstein, J. Loveday, M. A. Strauss, M. SubbaRau, D. H. Weinberg, J. E. Anderson, Jr., et al., *Astron. J.* **121** (2001), 2358.
- [16] S. A. Shectman, S. D. Landy, A. Oemler, D. L. Tucker, H. Lin, R. P. Kirshner, P. L. Schechter, *Astrophys. J.* **470** (1996), 172.
- [17] S. Cole, P. Norberg, C. M. Baugh, C. S. Frenk, J. BlandHawthorn, T. Bridges, R. Cannon, M. Colless, *Mon. Not. R. Astron. Soc.* **326** (2001), 255.
- [18] A. G. Riess, et al. astro-ph/0104455.
- [19] Y. Wang, *Astrophys. J.* **536** (2000), 531.
- [20] M. Hamuy, et al., *Astron. J.* **112** (1996), 239.